Force measurements on a cylinder with forced CF and IL motions in uniform current

The tests were carried out by Kristoffer Aronsen as a part of his PhD project at the Department of marine technology, NTNU, Trondheim, Norway. The main supervisor for Aronsen's PhD was professor Carl M. Larsen.

A full description of this work is found in Aronsen's PhD thesis, which can be downloaded from:

http://www.marin.ntnu.no/%7Ecallas/index_e.htm

Aronsen and a colleague (Svein Ersdal) during installation of the test pipe in the Marine Cybernetics Laboratory at NTNU, Trondheim

Principle sketch of test set-up

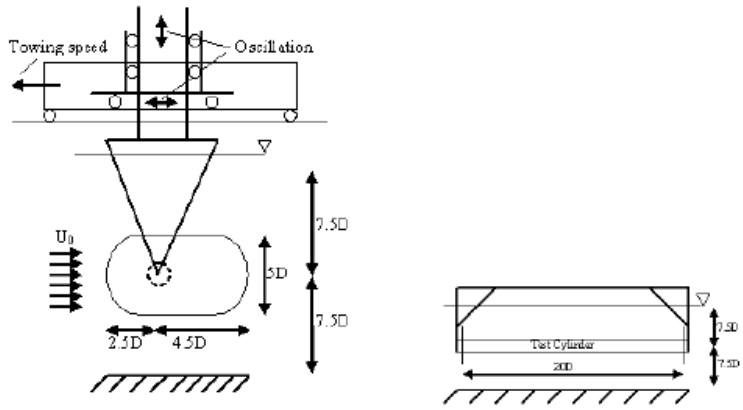

(a) Seen from port side (b) Front view

The test model was a 10cm diameter painted aluminium cylinder of 2m length. Hence, the L/D-ratio was 20 (see Figure 2b). The cylinder was installed in a yoke which in turn was attached to the motion simulator on the carriage. Model oscillations were achieved by oscillating the yoke horizontally (IL) and vertically (CF), while the ambient flow velocity was provided by a constant forward speed of the carriage. Microprocessor controlled servo motors gave the desired oscillation amplitudes, frequencies and phase difference between the vertical and horizontal directions. The cylinder was air filled with watertight plugs at both ends in order to keep the mass as low as possible. End plates were installed to eliminate 3D effects at the cylinder ends. The end plates were designed according to specifications given in Stansby (1974), see dimensions in Figure 2a.

Table 1 shows the characteristic parameters for the experimental setup.

Table 1
Characteristic properties for the experimental setup.

Diameter of cylinder	D	0.10	m
Length of cylinder	L	2.0	m
Mass of cylinder	M	9.68	kg
Cylinder volume	$V_{cyl} = L\pi D^2/4$	0.0157	m^3
Mass ratio	$M/\rho_w V_{cyl}$	0.62	-
Constant towing velocity	U_0	0.262	m/s
Reynolds number	Re	2.4E+04	-
Oscillation frequency, IL/CF	$f_{osc,IL/CF}$	0.85 / 0.43	Hz
Oscillation amplitude, IL/CF	$(\frac{A}{D})_{IL}$ / $(\frac{A}{D})_{CF}$	0.15 / 0.30	-

All components of the PIV system were mounted onto the main towing carriage and experienced the same mean towing velocity as the test cylinder. I.e. the PIV apparatus was fixed relative to the 2 dof forced motion of the cylinder. Hence the far field mean flow from PIV system point of view is the towing velocity of the carriage. Figures 3 and 4 show top and side view sketches of the PIV apparatus. In these sketches, the laser sheet is marked green, and the measurement plane is red.

The PIV equipment was situated downstream of the test cylinder. Hence the laser was shooting directly upstream to the cylinder, illuminating a vertical plane in the cylinder wake. As seen in Figures 3 and 4, two underwater probes contain camera, lens and mirror. Cameras are viewing the measurement plane from positions downstream and well to each side of the test cylinder. Camera position was determined mainly by size and shape of the desired measurement plane, optimum angle for stereoscopic PIV, as well as the demand of keeping the wake unaffected by the presence of PIV equipment. 2D-results presented here are based on data from one camera only. Cylinder motion starting point was set such that a portion of the cylinder would be visible in the measurement area at all times during experiments. The measurement area extends $3.52 * D$ in the CF direction and $5.07 * D$ in the IL direction.

The present system uses a Nd:YAG pulsed laser with two cavities, capable of 100 Hz double pulse at 50 mJ/pulse. The laser was run in double pulsed

Four conditions have been tested. These are pure IL and pure CF oscillation and two "figure of eight" cases with opposite orbital direction. The characteristic parameters for the four cases are:

$\hat{f}_{IL} = 0.325$, $\hat{f}_{CF} = 0.163$, $(\frac{A}{D})_{IL} = 0.15$, $(\frac{A}{D})_{CF} = 0.30$

The nondimensional frequency, $\hat{f}_{IL/CF}$ is defined as $\hat{f}_{IL/CF} = \frac{f_{osc,IL/CF} D}{U_0}$. The orbitals of the two "figure of eight" cases were constructed by Eqn. (1):

$$\begin{aligned} IL: \ x(t) &= A_{IL} \cdot \sin(2\pi f_{osc,IL} \cdot t + \alpha) \\ CF: \ z(t) &= A_{CF} \cdot \cos(2\pi f_{osc,CF} \cdot t) \end{aligned} \tag{1}$$

The index IL/CF means that the parameter or equation is valid for both IL and CF direction. The two "figure of eight" cases are illustrated in Figure 6. The important difference between the two cases is the orbital direction relative to the flow, referred to as current in the figure. It is seen that for the case $\alpha = 0$ the cylinder motion follows the flow direction at the dead end of CF motion, while the cylinder motion is opposite the flow direction for the $\alpha = 180$ case.

Definition of hydrodynamic coefficients and the procedure for calculation of the coefficients from measurements are given. The hydrodynamic coefficients are based on the steady-state region, see Figure (5), of the time series.

The drag coefficient is defined as:

$$C_D = \frac{1}{T}\int_t^{t+T} \frac{F_{IL}(t)}{\frac{1}{2}\rho D L U_0^2} \tag{2}$$

where F_{IL} is force in IL direction and T is taken as an integer number of oscillation periods.

The dynamic excitation coefficient is defined as:

$$C_{e,IL/CF} = \frac{F_{hydro,0,IL/CF}\sin(\phi)}{\frac{1}{2}\rho D L U_0^2} \tag{3}$$

Where $F_{hydro,0,IL/CF} sin(\phi)$ is the oscillating force in phase with velocity, in IL or CF direction. This coefficient is analogous to the C_{L_V} coefficient that has been used when reporting results from pure CF experiments, ref. Gopalkrishnan (1993) and others.

The added mass coefficient is defined as:

$$C_{a,IL/CF} = \frac{F_{hydro,0,IL/CF}\cos(\phi)}{\frac{\pi D^2}{4}\rho L a_0} \tag{4}$$

The added mass coefficient is based on the force in phase with acceleration divided by the acceleration amplitude of the harmonic oscillation, a_0, and normalized with respect to the mass of the displaced water.

When dealing with 2dof oscillations it has been found that there are significant hydrodynamic forces at multiples of the oscillation frequency. In order to quantify these forces a total dynamic force coefficient, $C_{t,n,IL/CF}$, of order n is defined. Index n indicates which multiple of the oscillation frequency the coefficient refers to. The coefficient is defined as follows:

$$C_{t,n} = \frac{\sqrt{a_n^2 + b_n^2}}{\frac{1}{2}\rho D L U_0^2}$$

where

$$a_n = \frac{2}{T}\int_t^{t+T} F_{hydro}(t)\cos(n\omega_0 \cdot t)dt$$

and

$$b_n = \frac{2}{T}\int_t^{t+T} F_{hydro}(t)\sin(n\omega_0 \cdot t)dt$$

An rms-coefficient, C_{RMS}, has been defined for the total hydrodynamic force:

$$C_{RMS} = \frac{\sqrt{2 \cdot \frac{1}{n}\sum_{t=1}^{n}(F_{hydro,t} - \bar{F}_{hydro})^2}}{\frac{1}{2}\rho D L U_0^2} \tag{8}$$

where $\bar{F}_{hydro}$ is the mean value of the hydrodynamic force.

The rms-coefficient is linked to the magnitude of the oscillating force, but does not refer to a given oscillation frequency or phase component relative to motions. The rms-coefficient is calculated for the oscillating force both in IL and CF direction.

The hydrodynamic force has been decomposed into one component in phase with velocity, $F_{hydro,0}\sin(\phi)$, and one component in phase with acceleration, $F_{hydro,0}\cos(\phi)$. The following definitions apply (ref. Vikestad (1998)):

$$F_{hydro,0}sin(\phi) = \frac{2}{T\omega_{osc}x_0}\int_t^{t+T} F_{hydro}(t)\cdot\dot{x}(t)dt \tag{11}$$

$$F_{hydro,0}cos(\phi) = \frac{2}{T\omega_{osc}^2 x_0}\int_t^{t+T} F_{hydro}(t)\cdot\ddot{x}(t)dt \tag{12}$$

where $\dot{x}(t)$ and $\ddot{x}(t)$ refers to the velocity and acceleration signal respectively and x_0 is the displacement amplitude.

Table 2
Hydrodynamic coefficients CF

Case	C_D	U_{C_D}	$C_{e,CF}$	$U_{C_{e,CF}}$	$C_{a,CF}$	$U_{C_{a,CF}}$
1dof CF , SB	1.725	0.067	0.648	0.027	3.180	0.123
1dof CF , Port	1.640	0.061	0.640	0.026	3.202	0.115
$\alpha = 0$, SB	1.662	0.065	-1.384	0.073	3.922	0.221
$\alpha = 0$, Port	1.653	0.058	-1.460	0.056	4.192	0.155
$\alpha = 180$, SB	1.956	0.079	0.916	0.036	3.171	0.126
$\alpha = 180$, Port	1.962	0.074	0.927	0.034	3.249	0.117

Table 3
Hydrodynamic coefficients IL

Case	C_D	U_{C_D}	$C_{e,IL}$	$U_{C_{e,IL}}$	C_{aIL}	$U_{C_{a,IL}}$
1dof IL, SB	1.866	0.056	-0.150	0.008	0.426	0.028
1dof IL, Port	1.899	0.109	-0.195	0.014	0.360	0.066
$\alpha = 0$, SB	1.662	0.050	-0.193	0.008	-0.117	0.031
$\alpha = 0$, Port	1.653	0.095	-0.209	0.012	-0.159	0.034
$\alpha = 180$, SB	1.956	0.062	0.105	0.004	0.357	0.024
$\alpha = 180$, Port	1.962	0.115	0.063	0.005	0.322	0.063

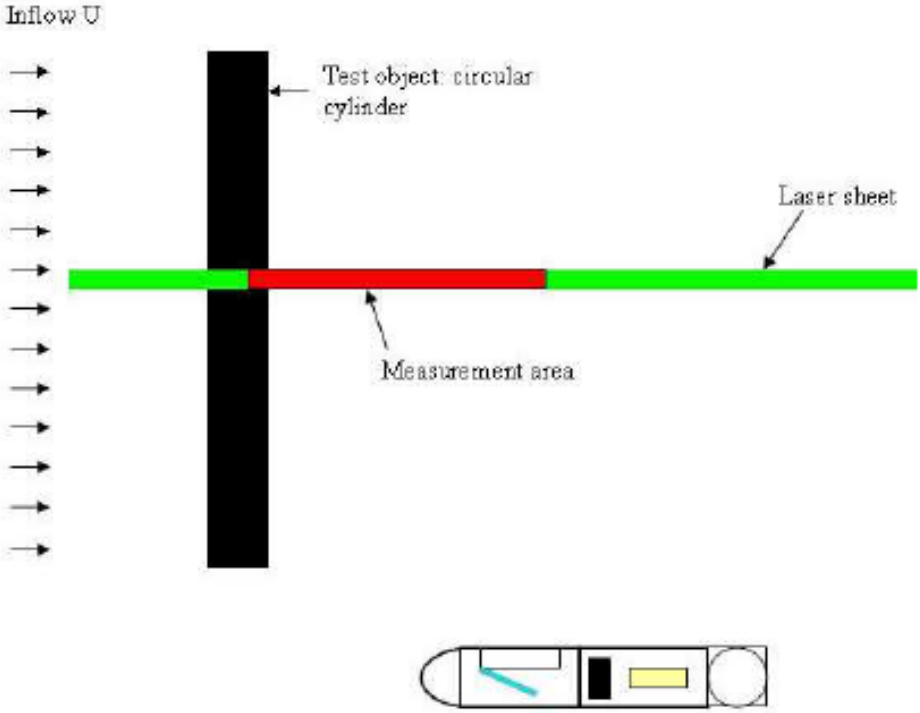

Fig. 3. Top view sketch of PIV apparatus. Sketch is not to scale.

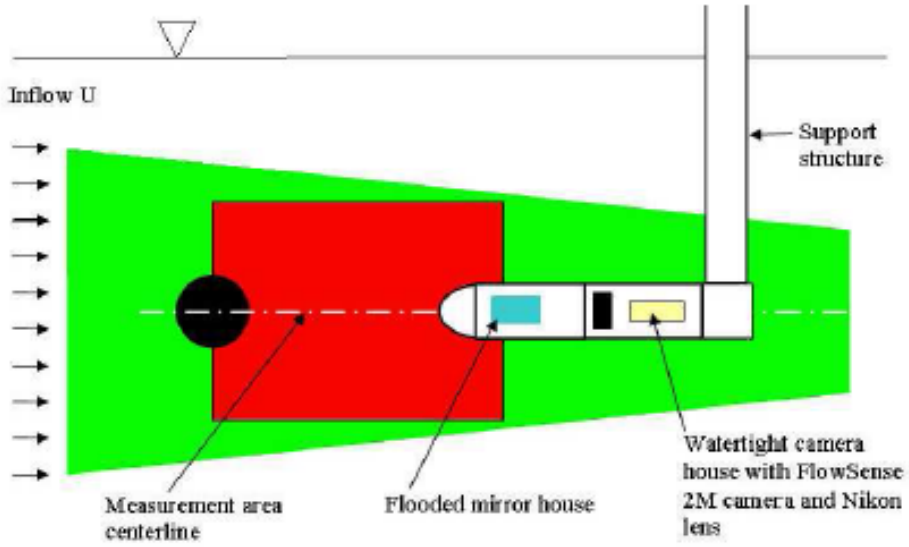

Fig. 4. Side view sketch of PIV apparatus. Sketch is not to scale.

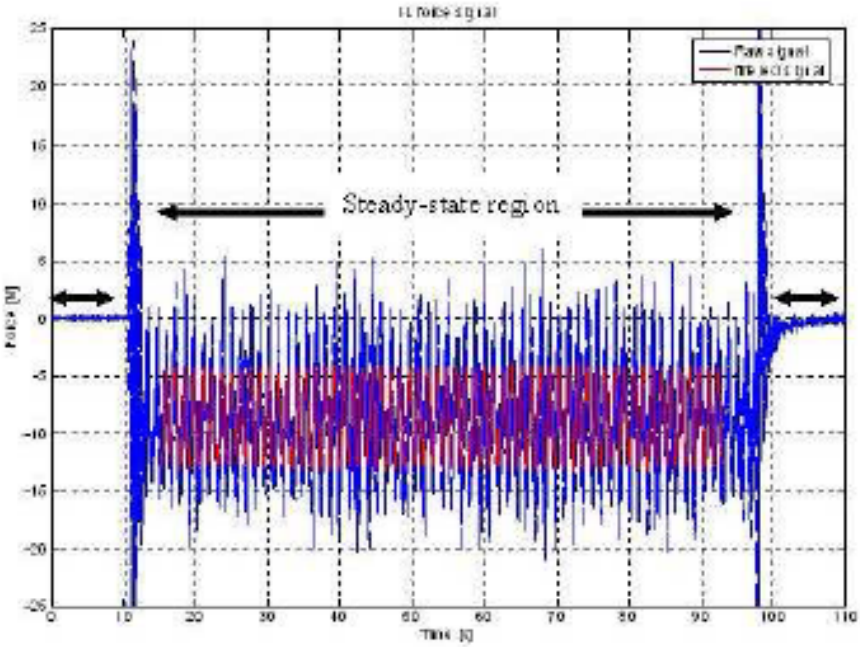

Fig. 5. Time series of measured IL force, raw signal and filtered signal

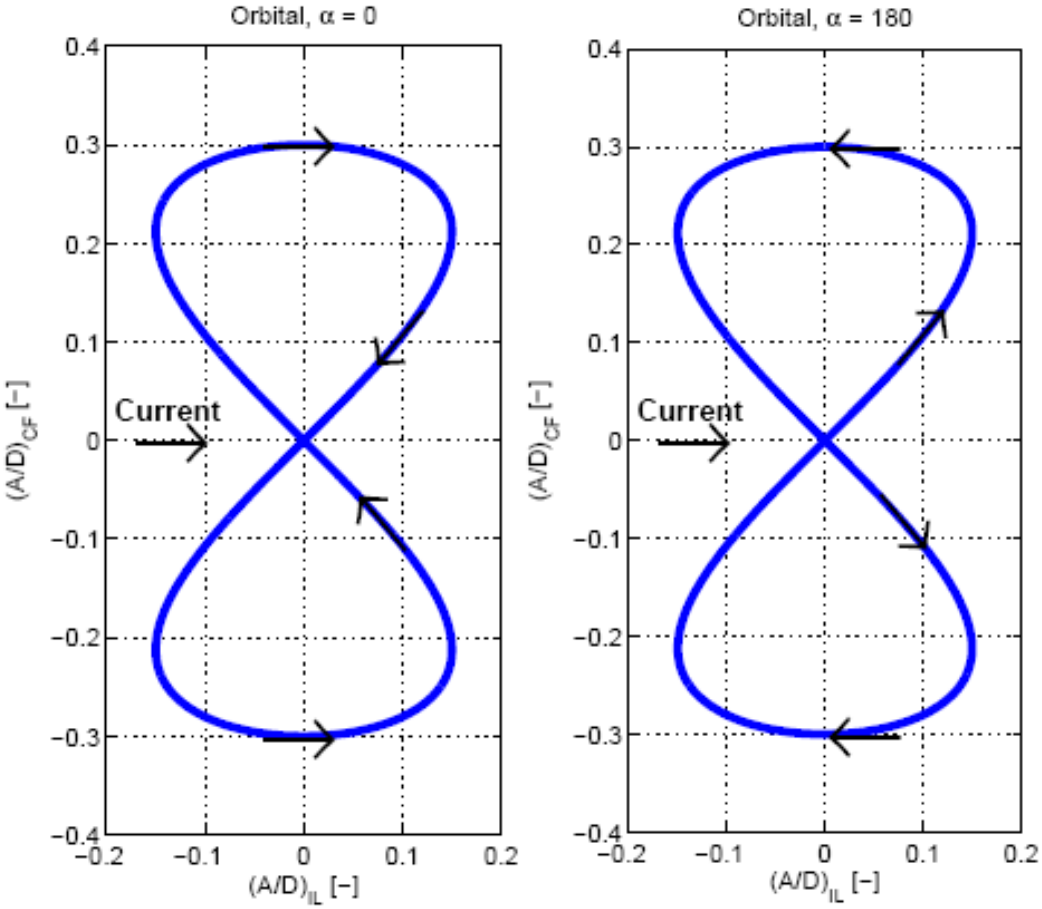

Fig. 6. ILLUSTRATION OF ORBITAL DIRECTION

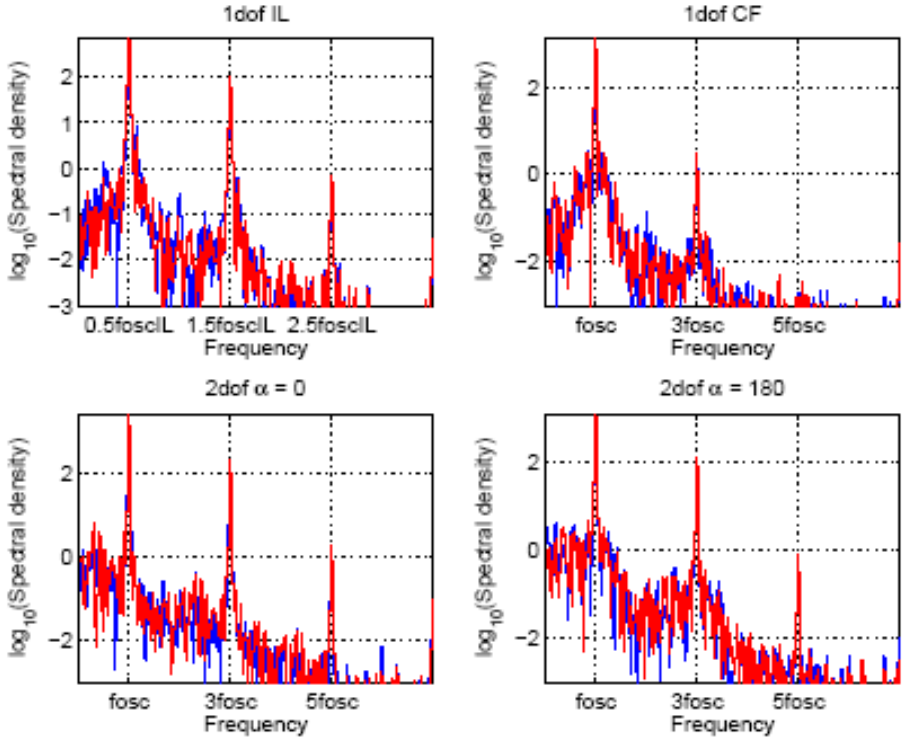

Fig. 7. POWER SPECTRUM OF CF FORCE. BLUE LINE FOR STARBOARD RESULTS AND RED LINE FOR PORT SIDE RESULTS

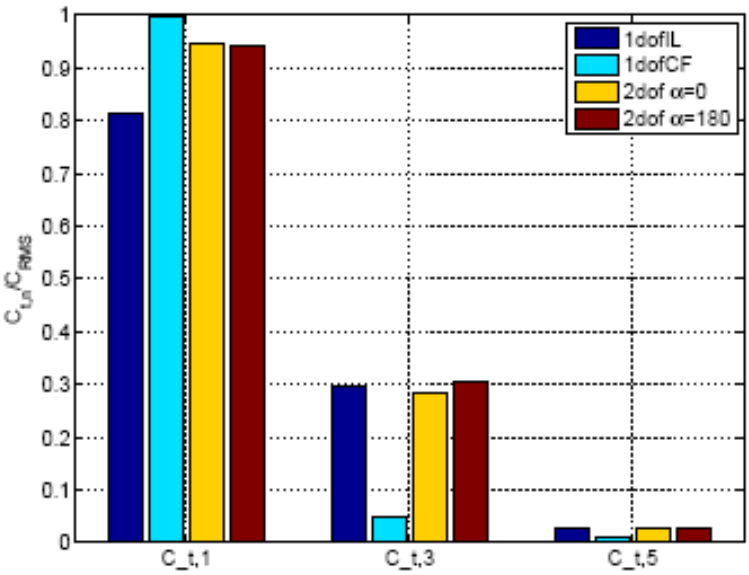

Fig. 8. TOTAL DYNAMIC FORCE COEFFICIENTS RELATIVE TO THE RMS COEFFICIENT. CF DIRECTION

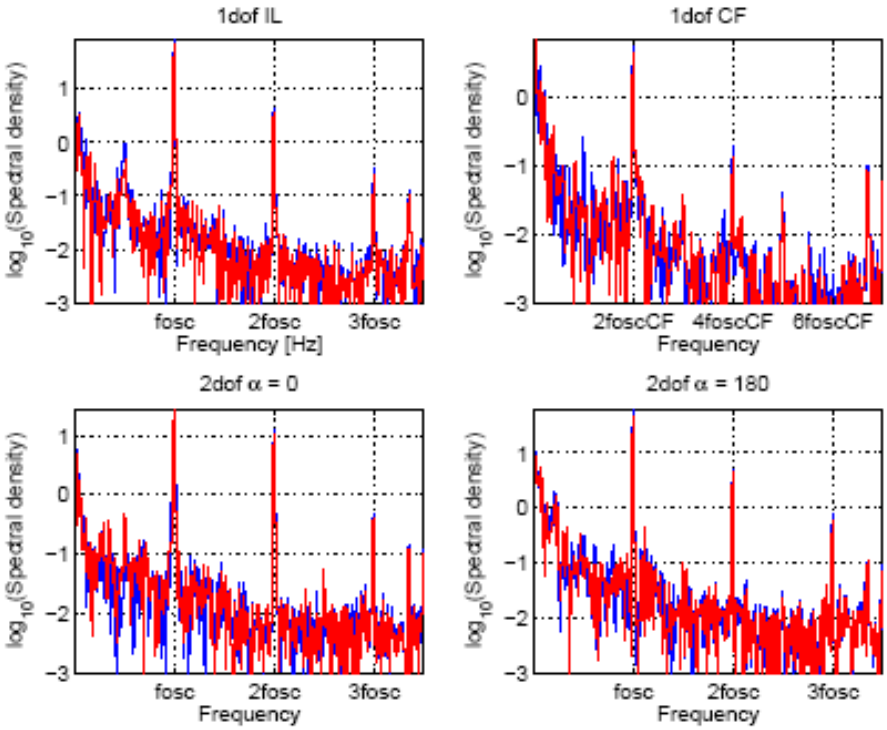

Fig. 9. POWER SPECTRUM OF IL FORCE. BLUE LINE FOR STARBOARD RESULTS AND RED LINE FOR PORT SIDE RESULTS

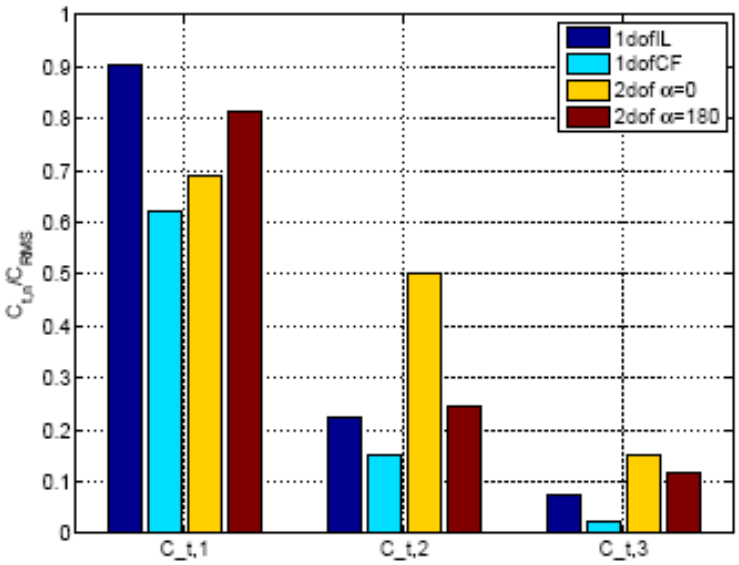

Fig. 10. TOTAL DYNAMIC FORCE COEFFICIENTS RELATIVE TO THE RMS COEFFICIENT. IL DIRECTION

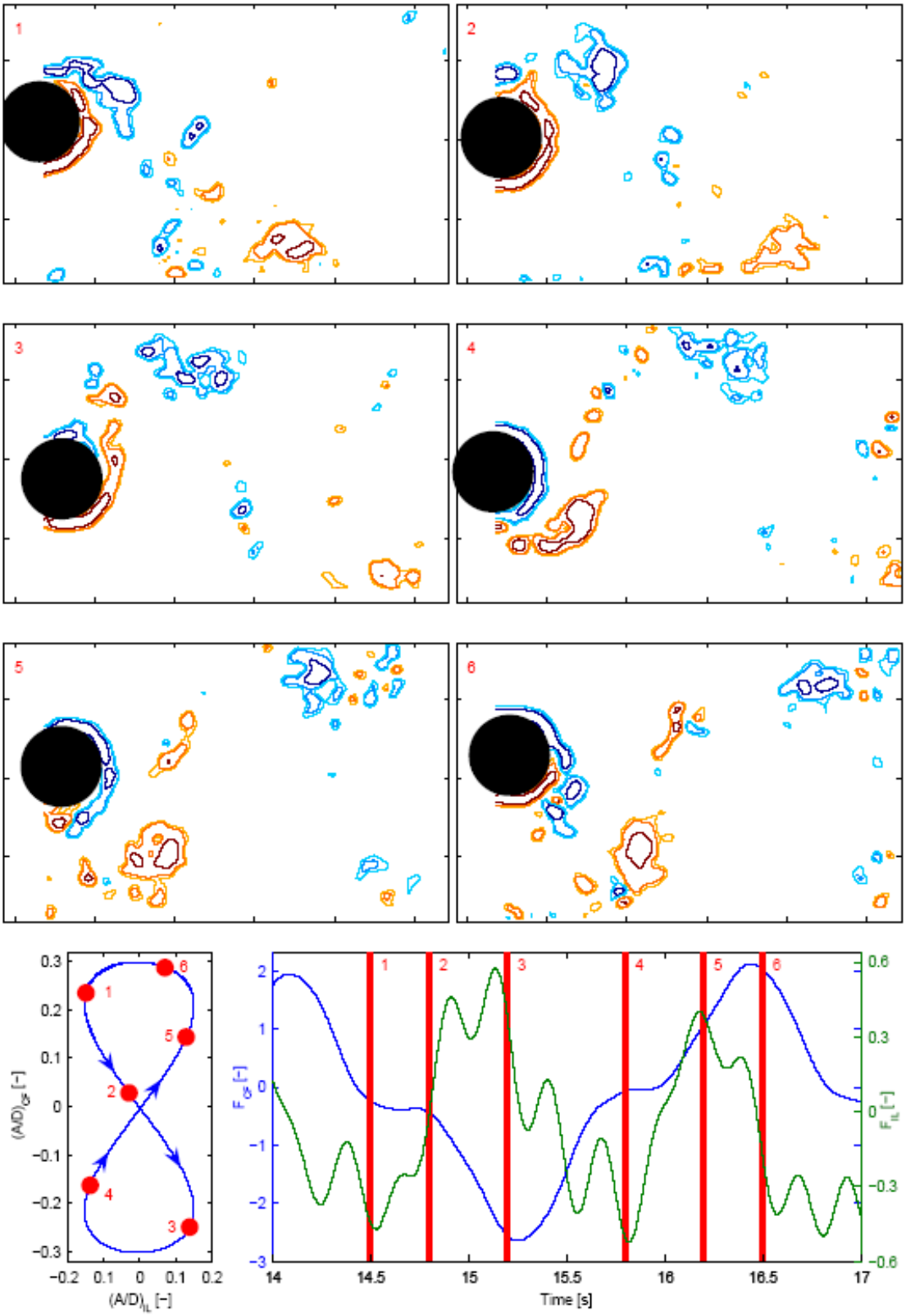

Fig. 11. PIV RESULTS FOR $\alpha = 180$

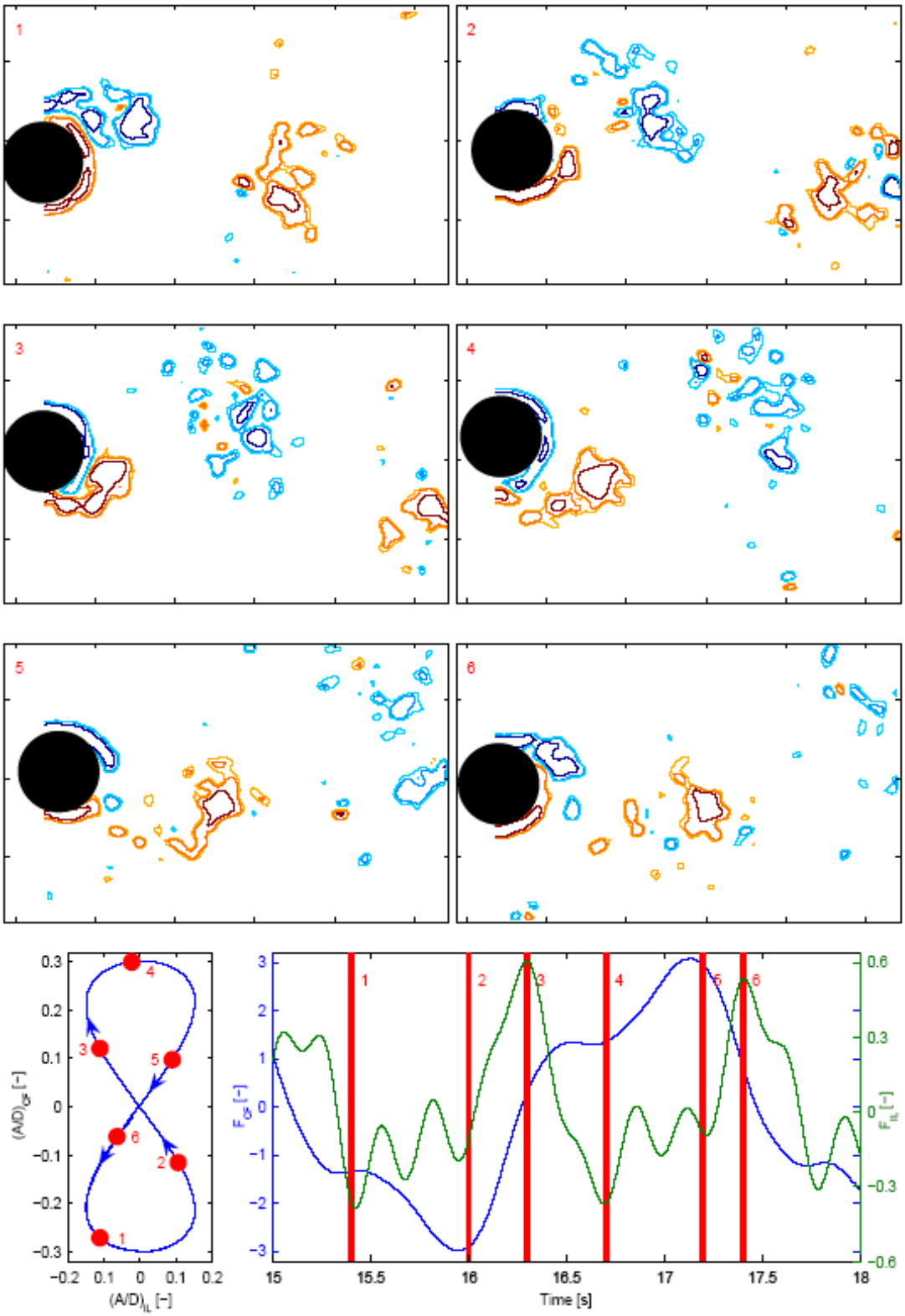

Fig. 12. PIV RESULTS FOR $\alpha = 0$